

Charge States of Heavy-Ion Beams Passing through Gases

P. M. STIER, C. F. BARNETT, AND G. E. EVANS*

Oak Ridge National Laboratory, Oak Ridge, Tennessee

(Received July 19, 1954)

Measurements are reported of the fraction of an ion beam in the various charge states ($-1, 0, +1, +2$) after equilibrium has been established between competing electron capture and loss reactions. The ions H^+ , He^+ , N^+ , Ne^+ , and A^+ were passed through the gases hydrogen, helium, nitrogen, oxygen, air, neon, and argon. The energy range studied was 20 kev to 250 kev. Under conditions of equilibrium between the singly ionized and neutral states, the velocity dependence of the charge ratios is given by $\sigma_{01}/\sigma_{10} = K_1 v^m$, where σ_{if} is the cross section for the transition between initial charge i and final charge f , v is the velocity, and K_1 and m are constants for each ion-stopping gas combination. The corresponding charge ratio for equilibrium between doubly and singly ionized states is given by $\sigma_{12}/\sigma_{21} = K_2 (v - v_c)^m$, where K_2 , v_c , and m are constants for each ion-stopping gas combination. The values of the constants v_c and m are tabulated. Negative ions are detectable only in the hydrogen beams. They constitute approximately 1 percent of the beam at 30 kev, and decrease in number rapidly at higher energies.

I. INTRODUCTION

AN important process by which low-energy heavy particles lose energy in passing through matter is charge exchange. For each electron capture and subsequent loss, the minimum energy loss by the incident particle is the ionization energy of the atoms of the stopping material. Also, the average charge of the particle beam (determined by charge exchange) influences the rate of energy loss by ionization and excitation because of the charge dependence of these cross sections.

The subject of charge exchange has been reviewed by Ruchardt¹ and more recently very useful summaries have appeared by Massey and Burhop² and by Allison and Warshaw.³ The capture and loss of electrons by protons have been studied in gases³ and in metal foils,^{4,5} and the electron capture and loss cross sections have been measured in hydrogen^{6,7} and air.⁸ Also, the charge exchange reactions have been studied for helium ions at high energies using natural alpha-particle sources,^{9,10} and at low energies by Meyer,¹¹ Rudnick,¹² and others.³ More recently, charge exchange for helium ions in gases has been investigated by Snitzer¹³ in the energy range 100 to 480 kev, and in metals by Dissanaïke¹⁴ from 0.13 to 1.1 Mev. Measurements of charge exchange for ions heavier than helium are restricted almost

entirely to energies less than 10 kev,² except for the work with fission fragments at much higher energies.

The present paper reports the results of measurements made of the fraction of a particle beam in each of the possible charge states after passage through a gas target which is sufficiently thick for equilibrium to be established between competing capture and loss reactions. These measurements have been made for each of the ions H^+ , He^+ , N^+ , Ne^+ , and A^+ passing through the stopping gases hydrogen, helium, nitrogen, oxygen, neon, and argon. Subsequent papers will report

- * On leave to National Carbon Company, Cleveland, Ohio.
¹E. Ruchardt, *Handbuch der Physik* (J. Springer, Berlin, 1933), Vol. 22, No. 2, p. 103.
²H. S. W. Massey and E. H. S. Burhop, *Electronic and Ionic Impact Phenomena* (Oxford University Press, London, 1952), Chap. VIII, Sec. 6.
³S. K. Allison and S. D. Warshaw, *Revs. Modern Phys.* **25**, 779 (1953).
⁴T. Hall, *Phys. Rev.* **79**, 504 (1950).
⁵J. A. Phillips, *Phys. Rev.* **91**, 455(A) (1953).
⁶J. H. Montague, *Phys. Rev.* **81**, 1026 (1951).
⁷F. L. Ribe, *Phys. Rev.* **83**, 1217 (1951).
⁸H. Kanner, *Phys. Rev.* **84**, 1211 (1951).
⁹G. H. Henderson, *Proc. Roy. Soc. (London)* **A109**, 157 (1925).
¹⁰E. Rutherford, *Phil. Mag.* **47**, 277 (1924).
¹¹H. Meyer, *Ann. Physik* **37**, 69 (1940).
¹²P. Rudnick, *Phys. Rev.* **38**, 1342 (1931).
¹³E. Snitzer, *Phys. Rev.* **89**, 1237 (1953).
¹⁴G. A. Dissanaïke, *Phil. Mag.* **44**, 1051 (1953).

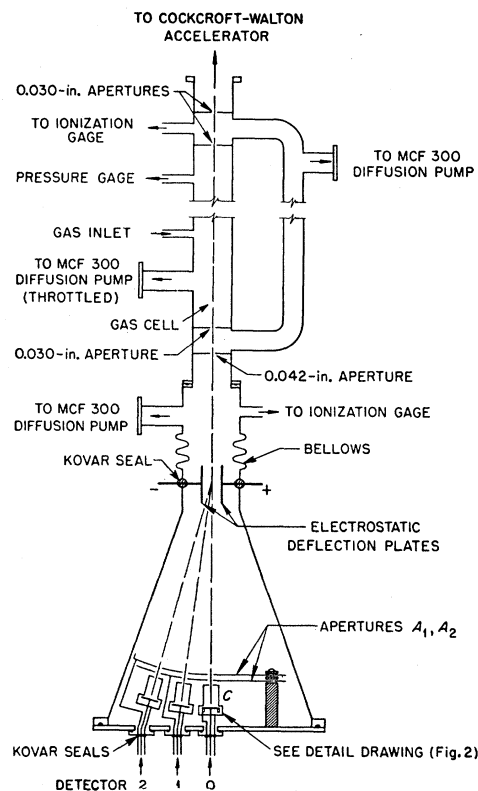


FIG. 1. Schematic drawing of the experimental apparatus.

measurements of the separate electron loss and capture cross sections for these incident ions and stopping gases. It is the purpose of this series of experiments to present a unified, consistent set of data from which an interpretation of the phenomena of charge exchange may be given in terms of the various pertinent parameters (mass, velocity, ionization potential, etc.).

II. DESCRIPTION OF APPARATUS

A. General

The output of a Phillips Ionization Gauge type ion source¹⁵ was accelerated in the ORNL heavy-ion Cockcroft-Walton accelerator. The desired ion mass was deflected by a stabilized analyzing magnet through an angle of 15 degrees and passed through the windowless gas cell shown schematically in Fig. 1. The gas cell was 18.0 inches in length and had an inside diameter of 1.13 inches. The beam entrance apertures were 0.030 inch and the exit apertures were 0.030 inch and 0.042 inch, as shown. The differential pumping properties allowed pressures of 0.2 mm Hg to be established in the gas cell without appreciably altering the pressure in the accelerator or electrostatic analyzer. The pressure in these regions was ordinarily between 0.8 and 1.0×10^{-5} mm Hg. The closely collimated particle beam which emerged from the gas cell, was electrostatically analyzed into the various charged components.

Differential pumping instead of foil windows was necessary because the range of the heavier ions used (e.g. A^+) at these energies is less than, or comparable to, the thickness of conveniently produced and handled foils.

The energy of the ions from the PIG source was within 100 ev of the applied plasma voltage. The current

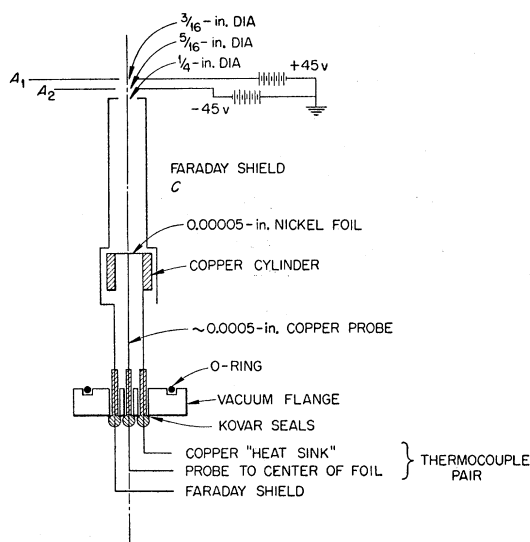


FIG. 2. Schematic drawing of the neutral (No. 0) detector.

¹⁵ Barnett, Stier, and Evans, Rev. Sci. Instr. 24, 394 (1953).

through a precision 600-megohm high-voltage resistor connected from the ion source anode to ground was used to measure the incident particle energy. The overall ion energy was held constant to within 0.02 percent of the desired value over long periods of time by a regulator in the high-voltage terminal. In principle, this circuit is equivalent to a conventional regulator used in most constant-voltage supplies at low voltage. The plate resistance of a triode in series with the supply load is controlled through a high-gain stabilized dc amplifier by the error between a reference voltage and the voltage developed in a fraction of the precision 600-megohm resistor by the bleeder current.

In these experiments, only the approach and attainment of charge equilibrium in the particle beam is measured. Since the fraction of the beam in the various charge states is pressure independent at equilibrium, the pressure measurement need not be absolute. An Alphasatron Gage¹⁶ was used for convenient, approximate pressure measurements.

In order to reduce evacuation time and permit continuous flushing of the gas cell, a liquid nitrogen trapped diffusion pump was connected to the gas cell through a throttling valve (Fig. 1). During many of the charge equilibrium measurements the stopping gas flowed through the charge exchange chamber at a rate of approximately one cc/min by appropriate adjustment of the throttling valve. This procedure acted as a test for impurities in the stopping gas arising from inleakage or chamber outgassing.

As shown in Fig. 1, the detector chamber was connected to the analyzer by means of a bellows section. This allowed the neutral (No. 0) detector to be aligned with the neutral beam. Also, the short section of the vacuum chamber, through which the analyzer Kovar seals pass, could be rotated about the axis of the neutral beam (this detail is not shown in Fig. 1). The vacuum seal was maintained by a peripheral O-ring at each end. Thus, after correct alignment of the neutral detector, the analyzing plates were positioned so that the charged beams struck the center of detectors No. 1 and No. 2.

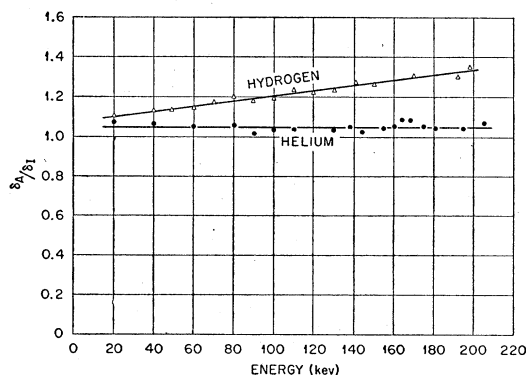


FIG. 3. Ratio of secondary electron emission coefficients for atoms to that for ions.

¹⁶ National Research Company, Cambridge, Massachusetts.

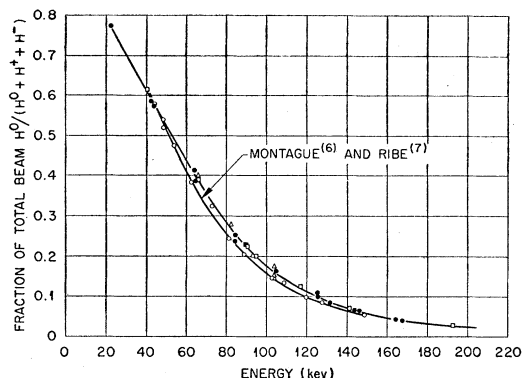


FIG. 4. Equilibrium fraction of hydrogen beam which is neutral in hydrogen gas. The following point designations are used: \circ = the results of Ribe (Ref. 7) and Montague (Ref. 6). \bullet = data taken with the apparatus shown in Figs. 1 and 2. \square = data taken using apparatus described in Sec. IVB. \blacksquare = data taken using apparatus described in Sec. IVB, with only neutrals incident on second charge exchange chamber. \triangle = data taken with apparatus described in Sec. II (Fig. 1) but using slow detectors described in Sec. IVA.

B. The Detectors

The neutral or undeflected particle beam impinges on a foil differential thermocouple similar to that described recently by Gardon.¹⁷ A schematic drawing of this detector is shown in Fig. 2. The thickness of the nickel foil was 0.00005 inch, yielding sensitivities of several microvolts per milliwatt with a time constant of about one second. As indicated, the collimated beam strikes near the center of the foil at the "hot" junction. The temperature of the relatively massive copper heat sink was independent of the beam because of the good conduction of the support structure. For the beam currents used in these experiments the temperature difference between the center of the foil and the heat sink was a few degrees. The output of this differential thermocouple was measured by a high-gain dc amplifier.

By applying appropriate potentials to the electrodes, the detector may be used either to measure the total incident charge (as a Faraday cup), or to measure the number of secondary electrons emitted by the foil (as a secondary electron detector). By using the thermocouple as a charge insensitive detector, the relative secondary emission for ions and atoms of the same mass and energy has been measured for this detector. The secondary electron emission for helium and hydrogen atoms was found to be somewhat higher than that for the corresponding ions, as shown in Fig. 3. These data are representative of the many simultaneous measurements of thermocouple response and secondary electron emission taken during the course of these experiments. They represent data taken under widely different experimental conditions of beam intensity, gas cell pressure, and alignment. Although the individual measurements deviate by several percent from the mean, no systematic change in the relative response

¹⁷ R. Gardon, Rev. Sci. Instr. 24, 366 (1953).

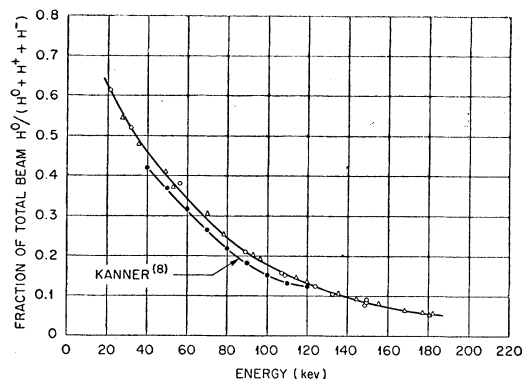


FIG. 5. Equilibrium fraction of hydrogen beam which is neutral in air. The point designations used are: \bullet = the results of Kanner (Ref. 8). \triangle = data taken with apparatus shown in Figs. 1 and 2. \circ = data taken with the apparatus described in Sec. IVB.

for ions and atoms could be detected. Corresponding plots for the ions and atoms of argon, neon, and nitrogen showed that within the limits of measurement, the secondary electron emission was independent of the particle charge. It should be pointed out that this observed relative secondary electron emission is for the foil surface conditions present in this experimental apparatus and may not be characteristic of a clean metal.

The secondary electron emission was found useful as a measure of the beam at the lower energies (less than 60 keV) where it was difficult to get sufficient response of the thermocouple. For calibration of the secondary emission, the pressure in the gas cell needed only to be high enough to neutralize an easily measured fraction of the beam. In general this could be much smaller than the pressure for charge equilibrium, so that attenuation caused by elastic scattering was not as severe.

The detectors No. 1 and No. 2 are similar to No. 0 except they do not contain a thermocouple. The apertures A_1 and A_2 , shown in Fig. 2, improve the efficiency of the secondary electron collection.

III. EXPERIMENTAL PROCEDURE

When using the equipment described in the preceding section, measurements of the fraction of the beam which was uncharged (after equilibrium between competing electron capture and loss reaction was established) were made as follows: After thoroughly flushing the gas cell with the target gas, a pressure of about 0.01 mm Hg was established in the gas cell. The particle beam emerging from the gas was allowed to strike the thermocouple detector and its response was recorded. Sufficient deflection voltage was applied to remove all charged particles from the beam and the response was again noted. These readings were repeated to minimize random errors caused by instability and errors in reading. Since the beam was usually stable to 1 percent during consecutive readings, results from successive

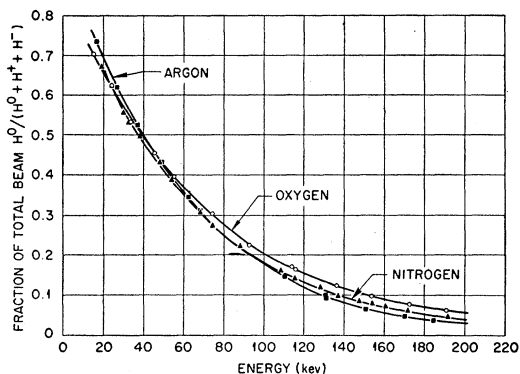


FIG. 6. Equilibrium fraction of hydrogen beam which is neutral in nitrogen, oxygen, and argon.

measurements agreed within 2 percent. All measurements were then repeated at a substantially different pressure and the results compared. If agreement was not within experimental error, additional gas cell pressures were established until the equilibrium charge distribution was attained. These steps were repeated at a sufficient number of incident ion energies to determine the dependence of the fraction of the particle beam which is neutral on the incident ion energy.

The measurement of the ratio of the number of doubly charged ions to the number of singly charged ions was made in one of two ways. For most of the measurements, the current to Faraday cup No. 1 was recorded as the analyzing voltage was varied to bring the charge one and charge two beams alternately into this detector. The other procedure was to read detectors No. 1 and No. 2 simultaneously. The results obtained by these two methods agreed within 2 percent. Repetition of the measurements at different pressures was again used as the test of equilibrium.

After completing the study of the positively charged components of the ion beams, it was felt that a search should also be made for negative ions in the beam emerging from the gas cell. This was accomplished by applying the deflection voltage necessary to bring the

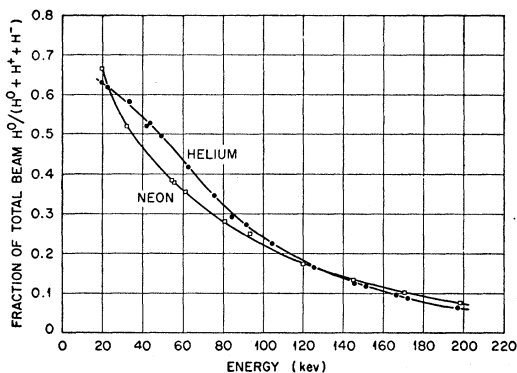


FIG. 7. Equilibrium fraction of hydrogen beam which is neutral in helium and neon.

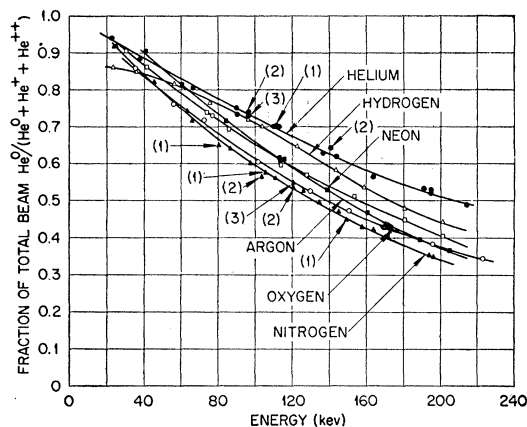


FIG. 8. Equilibrium fraction of helium beam which is neutral in various gases. The numbered points on the helium and nitrogen curves represent data taken by following methods: (1) using two slow thermocouples described in Sec. IVA, (2) using apparatus described in Sec. IVB, (3) using apparatus described in Sec. IVB with only neutral atoms incident on the second charge exchange chamber. All other points taken with apparatus described in Sec. II.

beam of charge +1 ions to detector No. 1 and then reversing the polarity of the deflecting voltage.

In this type of experiment it is assumed that the gas cell pressure is high enough so that equilibrium is established between competing capture and loss reactions (that is, the beam assumes an average, pressure-independent charge), but is low enough so that the energy degradation of the beam may be neglected. That this assumption is justified is evident from the fact that, particularly for H^+ and He^+ ions where elastic scattering is small, the pressure may be varied over a factor of ten with no change in charge distribution. For the heavier ions, where attenuation of the beam caused by elastic scattering is large, one finds that the average charge is pressure independent over a factor of three or four change in pressure. However,

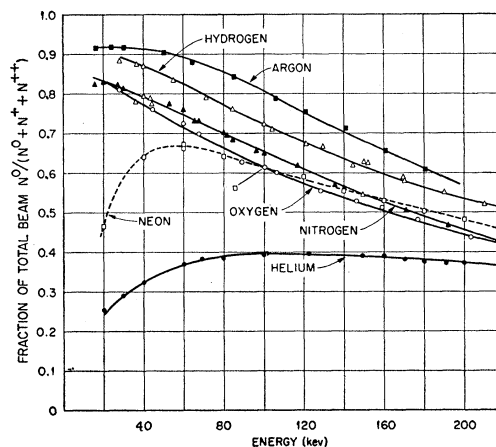


FIG. 9. Equilibrium fraction of nitrogen beam which is neutral in various gases.

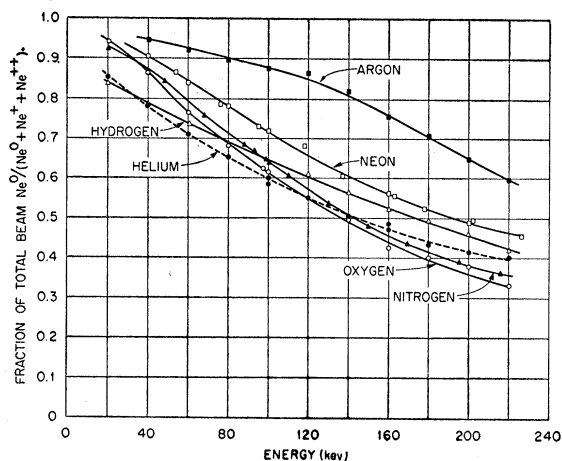


FIG. 10. Equilibrium fraction of neon beam which is neutral in various gases.

as the gas cell pressure is further increased, the fraction of the beam which is neutral begins to decrease slightly. This is in contrast to the expected behavior for a beam degraded in energy. This decrease may be associated with the relative elastic scattering of ions and atoms.

IV. OTHER EQUIPMENT AND PROCEDURES

In view of the rather large differences which often exist between the results of different workers in this field, it was felt that it would be wise to test for systematic errors because of the type of detector, gas cell geometry, and experimental procedure. For this purpose, during preliminary experiments, several such variations were made.

A. Detector Changes

The detectors No. 1 and No. 0 described in Sec. IIB were replaced with simple 0.003-inch copper-constantan wire thermocouples spotwelded to platinum foils $\frac{3}{8}$ inch

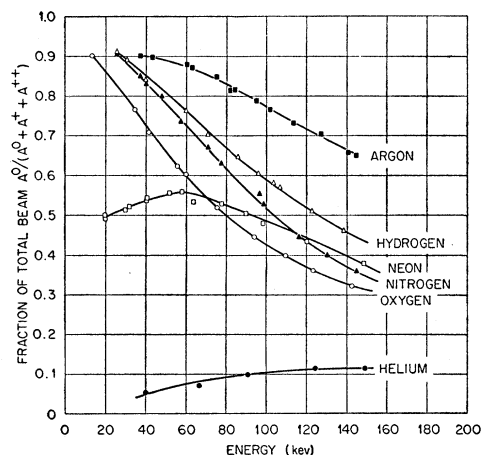


FIG. 11. Equilibrium fraction of argon beam which is neutral in various gases.

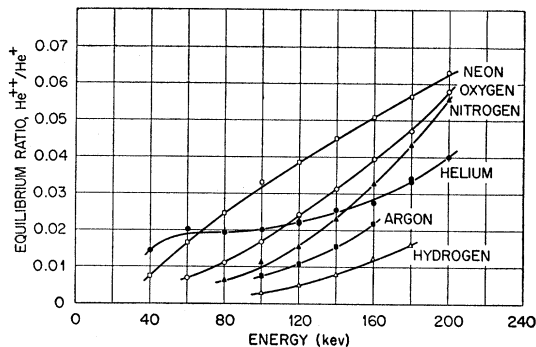


FIG. 12. Equilibrium ratio of He⁺⁺ to He⁺ in various gases.

in diameter and 0.001 inch thick. These thermocouples required approximately five minutes to reach equilibrium and proved to be identical in response to within 3 percent, the accuracy of measurement. This sensitivity measurement was made with the gas cell at high vacuum so that nearly all the beam was singly charged. As described above, the method of support of the detector chamber was such that either thermocouple could be placed at the "neutral beam position" to record the total beam, and by applying the analyzing voltage in the correct polarity, the singly charged component could be measured on the other thermocouple. This versatility allowed the equivalence of these thermocouples to be established and thus served as a test of the detectors described in Sec. IIB, which were used for most of the work described in this paper. Sample results obtained with these slow thermocouples are displayed in Figs. 4 and 8 for comparison with the results measured with the fast differential thermocouple.

B. Geometry Changes

In order to test for possible systematic errors caused by gas cell geometry or differential pumping apertures, a series of measurements of the neutral component of the beam were made on apparatus being assembled for measurements of electron loss cross sections to be described in a subsequent paper. This equipment con-

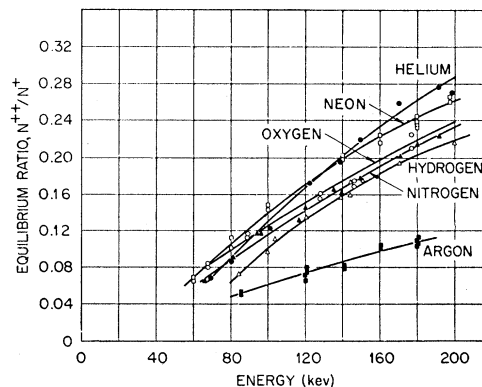


FIG. 13. Equilibrium ratio of N⁺⁺ to N⁺ in various gases.

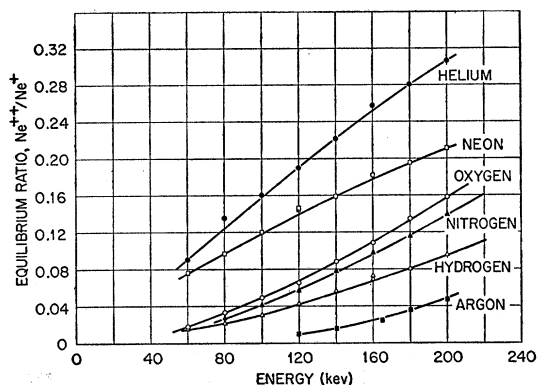


FIG. 14. Equilibrium ratio of Ne^{++} to Ne^+ in various gases.

sisted of two differentially pumped gas cells, each of which was followed by an electrostatic analyzer. With this arrangement, it was possible to make the particle beam incident on the second charge exchange chamber entirely uncharged, so that charge equilibrium is approached from an initially neutral beam rather than the customary singly charged beam. By definition, the results should be identical if equilibrium is established. For both of these gas cells, instead of using a differentially pumped "window," as described above, the entrance and exit apertures were canals, $\frac{1}{2}$ inch in length and $\frac{1}{16}$ inch in diameter. The pumping speed from the analyzing chambers was sufficient to maintain pressures of about 5×10^{-5} mm Hg. Only one detector was used since only the fraction of the particle beam, which was neutral, was measured. This was a differential thermocouple and Faraday cup similar to the described in Sec. IIB. For comparison, a few data taken with this apparatus are plotted in Figs. 4, 5, and 8.

V. ANALYSIS OF EXPERIMENTAL RESULTS

A. Relation of Charge Equilibrium to the Capture and Loss Cross Sections

The differential equations representing transitions between the possible charge states can be solved for the fraction of the particle beam in each state as a

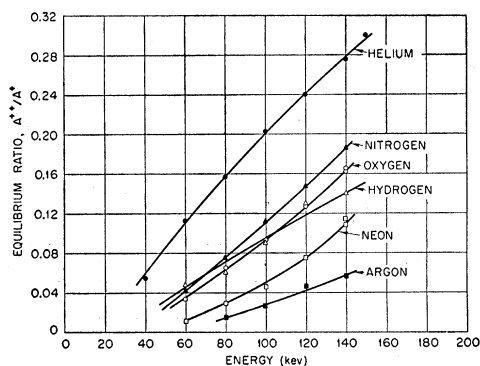


FIG. 15. Equilibrium ratio of A^{++} to A^+ in various gases.

function of the amount of stopping material traversed. As the amount of target material is increased, the fraction in charge state i approaches limiting values F_i . For the energies used in these experiments, three charge states, 0, +1, +2, are of importance and the corresponding equilibrium fractions, F_0, F_1, F_2 , are measured in these experiments. These can be expressed in terms of the cross sections as:¹⁸

$$F_0 = \sigma_{10}\sigma_{21}/D_0, \quad F_1 = \sigma_{01}\sigma_{21}/D_0, \quad F_2 = \sigma_{01}\sigma_{12}/D_0,$$

where $D_0 = \sigma_{01}(\sigma_{12} + \sigma_{21}) + \sigma_{10}\sigma_{21}$ and σ_{if} represents the cross section for transition from initial state i to final state f . The usual assumption has been made that the cross section for a collision in which two electrons are transferred is small. It is evident that

$$F_1/F_0 = n^+/n^0 = \sigma_{01}/\sigma_{10}; \quad F_2/F_1 = n^{2+}/n^+ = \sigma_{12}/\sigma_{21}.$$

B. Experimental Results

The results of the determinations of the fraction of the particle beam which was neutral at charge equilibrium are displayed in Figs. 4–11. In Figs. 4 and 5, the data for protons passing through hydrogen and air are compared with the results of other observers. The ratio of charge 2 to charge 1 components are given in Figs. 12–15.

The number of negative ions formed in the charge exchange chamber was below the detectable limit (about 0.1 percent of the total beam at 30 keV, 0.01 percent at 100 keV) for the incident ions He^+ , N^+ , Ne^+ , and A^+ . The energy dependence of the H^- component formed by the passage of protons through nitrogen is shown in Fig. 16.

The study of the negative component was only extensive enough to establish that, for the energy range investigated, no serious error was introduced by neglecting it in the computation of the neutral or positive fractions.

C. Errors

The measurement of the incident ion energy is believed to be correct to within 0.2 percent. The voltage dividing resistor between the ion source and ground was composed of precision wire-wound resistors. These were mounted within a structure which established a potential around each resistor appropriate for that resistor. This avoided errors in the calculated bleeder current caused by corona. As mentioned previously, the terminal regulator maintained the over-all ion energy constant to within 0.02 percent of the desired value.

The best test of the over-all stability of the ion source, energy, analyzing magnet supply, and detector amplifiers is the stability of the particle current measured at the detectors. Ordinarily, after a short startup period, this was stable to about 1 percent for the period

¹⁸ See, e.g., reference 3 for a rather complete derivation and discussion of these equations.

of time required for the series of measurements taken at each energy point.

As discussed above, in most cases, the rate of gas flow through the charge exchange chamber was increased to about an atmospheric cubic centimeter per minute in order to minimize the effect of impurity buildup caused by outgassing, inleakage, or the beam, in the cases of strong elastic scattering. The air used as stopping gas was dried and the carbon dioxide removed by Drierite, KOH, and P₂O₅. The other gases were good-grade compressed gas and were used as supplied except for being passed over a cold trap. For oxygen and argon the trapping agent was a dry ice-butyl cellulose mixture, and for the remaining gases liquid nitrogen was used.

The search for errors caused by gas cell geometry or detector properties has been described in Sec. IV. It should also be noted that during most of the experiments the cross section of the particle beam at the detector position was approximately $\frac{1}{8}$ inch in diameter, whereas the detector aperture and sensitive area were $\frac{5}{16}$ inch. Thus, a very definite plateau existed in a response *versus* detector position curve when secondary electron or positive ion detection was used. The corresponding curve for the differential thermocouple was of course somewhat rounded at the top. As described above, by appropriate detector positioning and adjustment of the deflecting voltage, a beam of particles of

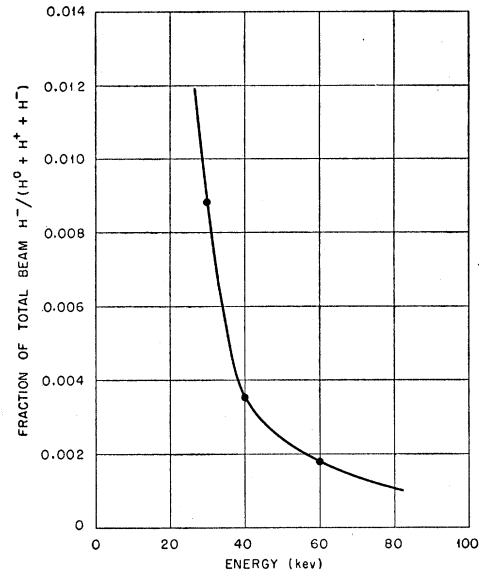
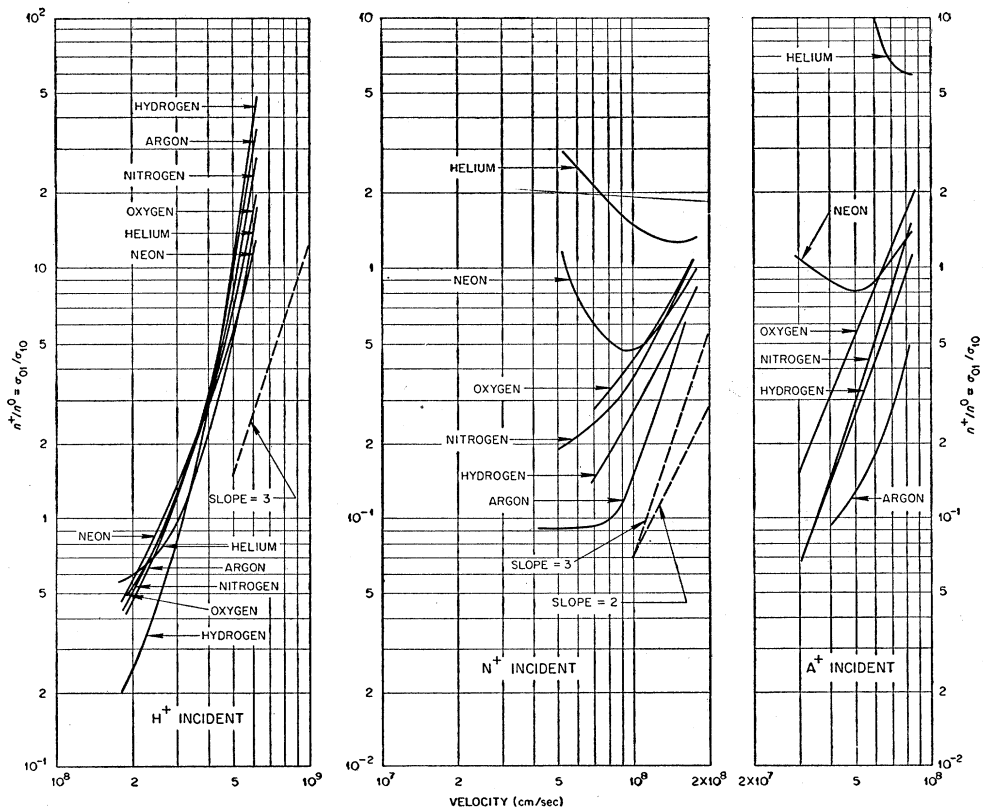


FIG. 16. Equilibrium fraction of hydrogen beam which is H⁻ in nitrogen.

charge +1 could be moved to each of the detectors. The agreement was within 2 percent.

The linearity of the electrometers used was measured to be within 1 percent and the thermocouple was linear to 1 percent over the very limited temperature range

FIG. 17. Ratio of loss to capture cross sections (σ_{01}/σ_{10}) for hydrogen, nitrogen, and argon ions in various gases.



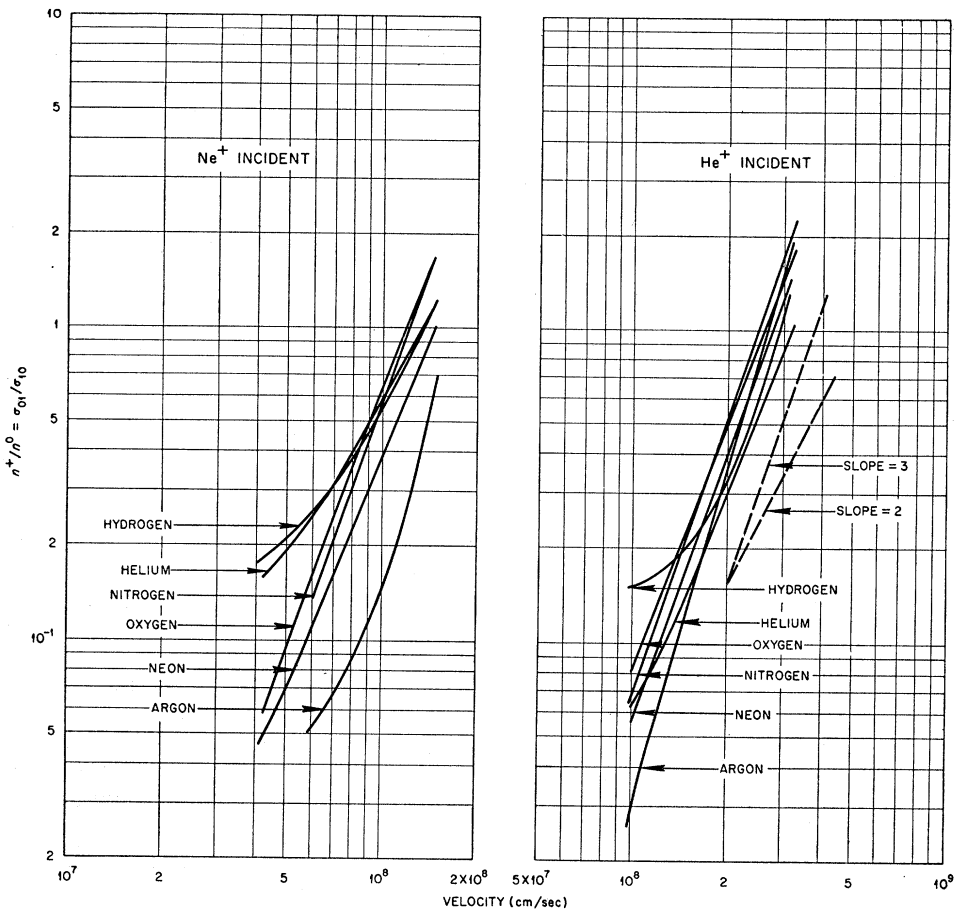


FIG. 18. Ratio of loss to capture cross sections (σ_{01}/σ_{10}) for helium and neon ions in various gases.

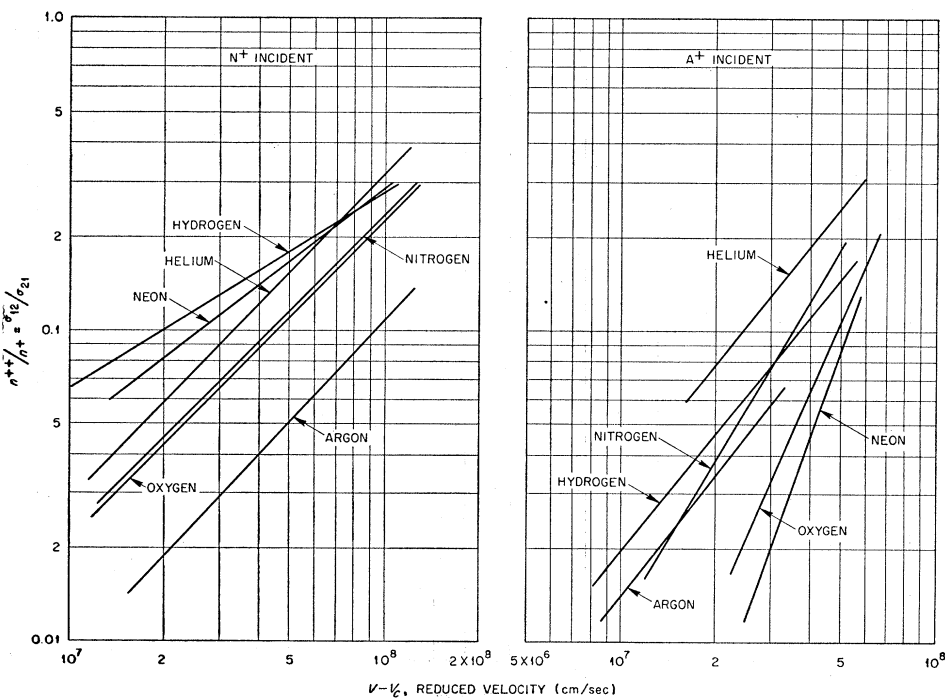


FIG. 19. Ratio of second loss to capture cross sections (σ_{12}/σ_{21}) for nitrogen and argon ions in various gases.

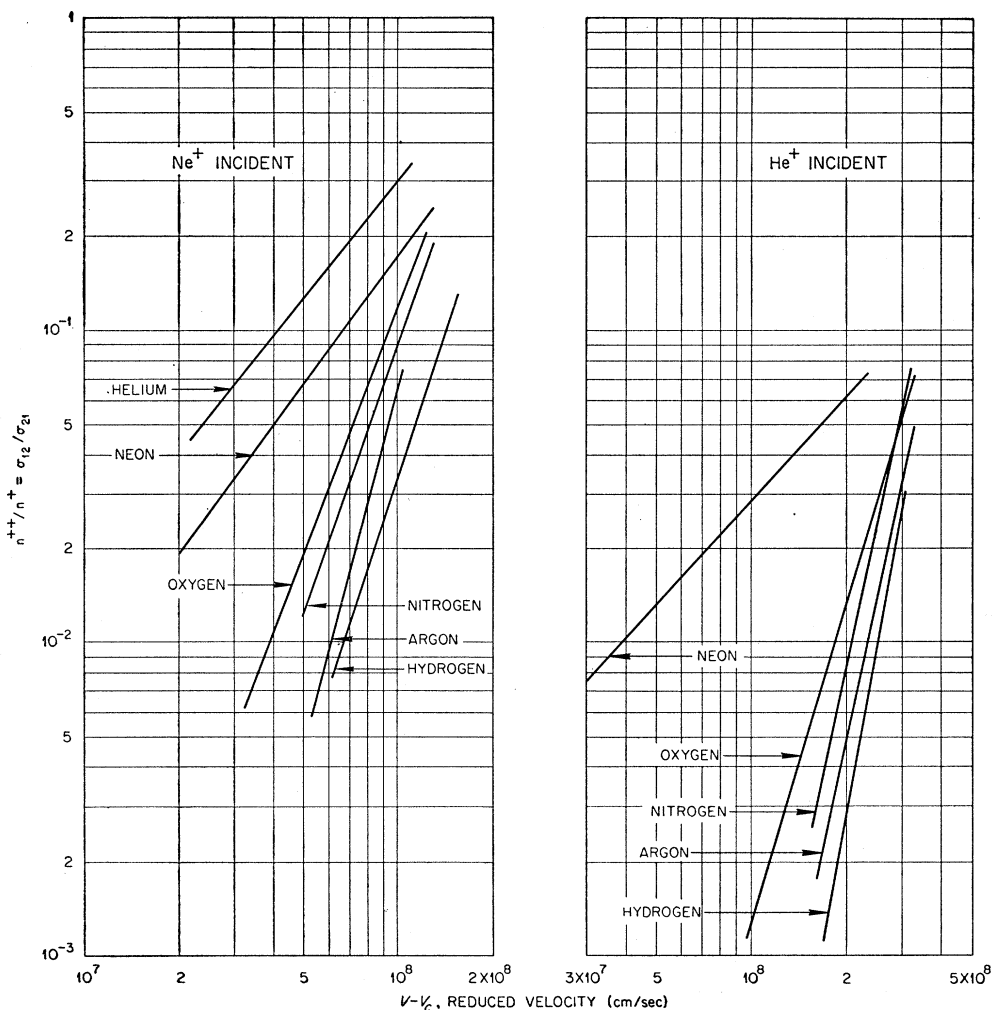


FIG. 20. Ratio of second loss to capture cross sections (σ_{12}/σ_{21}) for helium and neon ions in various gases.

used in these experiments. This is verified by the agreement between data taken for very different intensity ion beams.

The over-all error in the results is estimated to be not larger than 5 percent, and is probably less than this for much of the data. Because of the subtraction technique used for measurement of the neutral fraction of the beam, the accuracy is best when the beam is approximately equally divided between the charge states. In general the error is largest at the low energies because of decreased beam intensity and the consequent reliance on the secondary electron emission for beam measurements.

VI. DISCUSSION

The agreement between the present measurements and the results of Montague⁶ and Ribe⁷ for protons in hydrogen (Fig. 4) and of Kanner⁸ for protons in air (Fig. 5), while not exceedingly good, may be considered satisfactory. The equilibrium neutral fraction shown in Figs. 4 and 5 are calculated from their measured capture and loss cross sections.

Snitzer's reported results for the neutral fraction of a helium beam passing through hydrogen, helium, air, and argon are in each of these cases from 20 to 30 percent below the results shown in Fig. 8. Since the various tests described in Sec. IV indicated no systematic errors larger than the random error of 2 or 3 percent, no explanation can be given for this large discrepancy. It should be pointed out that the ratio of the number of doubly to singly charged ions in the helium beams (Fig. 12) is in good agreement with Snitzer's values, provided his lowest energy points for this ratio are disregarded. This provision seems justified since the doubly charged component for these points appears to be only slightly larger than his detectable limit.

In interpreting the results of experiments which measure the equilibrium charge ratio for heavy ions, it must be kept in mind that only the ratio of the electron capture and loss cross sections is determined, and that these cross sections are for different types of interactions, whose energy dependence is expected to

TABLE I. Values of the exponent m in the relation $\sigma_{01}/\sigma_{10}=K_1v^m$ for the various ion-gas combinations.^a

Ion Gas	Ion				
	H ⁺	He ⁺	N ⁺	Ne ⁺	A ⁺
H ₂	6.5	3.3	2.0	2.2	2.8
He	4.7	2.6	*	1.9	*
N ₂	5.4	2.9	2.2	2.9	3.3
O ₂	4.6	2.6	1.7	2.8	2.5
Ne	3.7	2.8	*	2.5	*
A	5.8	3.5	3.1	4.3	3.7

^a An asterisk indicates that the log-log plot has no straight line portion

differ. The electron loss is ionization of a fast atom by a target atom. Therefore, the loss cross section is expected to increase to a maximum and then decrease slowly at higher energies. The capture cross section is the cross section for the transfer of an electron from a target atom to a projectile ion. In this low energy region its behavior will be largely determined by the relative ionization potential of the target and projectile atoms. It is expected to decrease more rapidly than the loss cross section at higher energies.

As discussed in Sec. V(A), when it is assumed that the probability that two electrons are transferred in a single collision is negligible, the ratio of the number of particles in charge states +1 and 0 (or in +2 and +1) is the ratio of the cross sections for transitions between

TABLE II. Values of the "threshold velocity" v_c and the exponent m in the relation $\sigma_{12}/\sigma_{21}=K_2(v-v_c)^m$ for the various ion-gas combinations.^a

Ion Gas	m				Ion Gas	$v_c, \text{ cm/sec} \times 10^{-8}$			
	He ⁺	N ⁺	Ne ⁺	A ⁺		He ⁺	N ⁺	Ne ⁺	A ⁺
H ₂	5.7	0.6	3.0	1.3	H ₂	0.2	1.0	0	0.3
He	*	1.1	1.3	1.3	He	*	0.7	0.4	0.3
N ₂	4.7	1.0	2.8	1.7	N ₂	0.1	0.7	0.2	0.3
O ₂	3.4	1.0	2.7	2.3	O ₂	0	0.6	0.3	0.2
Ne	1.1	0.8	1.4	2.9	Ne	1.1	0.8	0.2	0.3
A	4.7	1.0	3.8	1.3	A	0	0.6	0.5	0.5

^a An asterisk indicates that the log-log plot has no straight line portion.

these states. The ratio σ_{01}/σ_{10} calculated from values read from the smooth curves in Figs. 4-11 are plotted as a function of the incident ion velocity in Figs. 17 and 18. It is seen that much of the experimental data are well represented in this energy range by formulas of the type $\sigma_{01}/\sigma_{10}=K_1v^m$, where v is the particle velocity and K_1 and m are empirically determined constants. The parameter m varies for the different incident ion-stopping gas combinations, and values are listed in Table I for each ion-gas combination for which the data could be represented by a straight line over a reasonable portion of the velocity range. The interesting behavior of the relatively easily ionized, heavy ions (nitrogen and argon) when passing through the gases of high ionization potential (helium and neon) is to be noted. As discussed above, the velocity dependence of the reactions involved is expected to differ and it would, therefore, seem that detailed discussion of the shapes of these curves should be deferred until the separate cross sections have been measured.

It is evident from Figs. 12-15 that in many cases the ratios of the cross sections for transitions between charge states +2 and +1 cannot be represented by a simple power law in velocity over the energy range studied since the curves do not extrapolate to $n^{2+}/n^+ = \sigma_{12}/\sigma_{21} = 0$ at zero energy. However, the data are well represented by formulas of the type

$$\sigma_{12}/\sigma_{21} = K_2(v-v_c)^m,$$

as is shown in Figs. 19 and 20. The empirically determined values for the constants m and v_c are shown in Table II. v_c corresponds to a "threshold velocity," below which there is very little probability of forming the doubly charged ion. Here again it is difficult to interpret the details of this table because of the unknown and different velocity dependence of the cross sections involved.

The authors wish to acknowledge helpful discussions with Doctors A. H. Snell and E. O. Wollan of the Oak Ridge National Laboratory physics staff, and with Dr. S. K. Allison of the University of Chicago.